Modelling a Human Transporter

Name(s)

Farhan Jarif (21024752)

Prabhjot Khera (21005282)

Cheran Selvarajah (21013444)

Sachin Gill (2099003)

Group#

23

Date

March 10th 2025

Course Number & Name

SYDE 351 – System Models

Instructor's Name

Charbel Azzi

Abstract

Automated control systems play crucial roles in sustaining stability and performance in most engineering applications. In this project, a human transporter was designed and analyzed using theoretical modeling and simulation. A mathematical model to predict system behavior and optimum control parameters were developed using MATLAB/Simulink to obtain optimal performance. Additionally, a physical model was built using SimulationX to compare to Simulink's numerical model. The aim was to create an efficient and stable transporter model, ensuring that our design meets both practical constraints and performance criteria.

Through iterative simulations, the system's response was simulated using different inputs and disturbances, adapting our approach based on differences between theoretical predictions and simulated outputs. The key findings included the significance of extremely precisely tuning the thrust force to optimize performance, in addition to the Simulink and SimulationX model having varying outputs for the same parameters. Through the step-by-step examination of these factors, many insights were gained about control system design and its applications in the real world. This report outlines the methodology, design decisions, and findings from this project.

Table of Contents

List of Figures

List of Tables

1 Introduction (1 page)

The project task was to model a human transporter. The transporter, more commonly known as a segway, is a device that is used to transport a person at low speeds and has a maximum speed of around 20 km/h. They are very common among commuters in the city and have recently become much more popular. The design is composed of two wheels attached by two axles to joints that allow them to both rotate and translate forward and backward. Unlike a bike where the wheels are in line with each other the segway has both wheels side by side similar to the two front wheels of a car. Depending on the model, the main controller component may be either between your legs and controlled by the sway of the user's legs or a tall handlebar that is then controlled by the user's hands. These segways are quite smart and have unique features. They contain a very advanced gyroscope that records the tilt of the device and can balance the Segway with various self-balancing features. The task at hand is to study the motion of the transporter specifically in one axis. For the project the segway will not be turning and will continue along one axis moving forward. The goal of the project is to model the transporter and to find all the ideal parameters which will keep the segway upright and help it travel for the longest distance before eventually toppling over. These parameters include a thrust force, and two different angle parameters. The fine tuning of these parameters will be key to maximizing the displacement and is a key aspect to the project. The problem will then be modelled using SimulationX to model what the behavior of the segway would look like in real life. The model will contain a simplified model of the base and handlebars and will also have a representation of a human riding the segway.

2 Background (1 page)

Segways are the most well-known brands to make human transporters as seen in the project. These Segways are composed of many internal systems. One system being the electric motor. Given that Segway's can travel a decent distance while carrying an adult, they have motors with capacities ranging from 700 to 1500 watts [1]. There are also many sensors within the human transporter, these sensors measure a variety of things from speed to incline. This data is then sent to the gyroscope which is a key component of the Segways self-balancing function [2]. In these personal transporter devices, the Gyroscope is typically a small silicon plate that vibrates depending upon which axis the device is tilted to. Once the data is received by the gyroscope, it then sends out the data according to the control board. The segway can attain the pitch which is the angle that it is tilting from an upright position and the pitch rate as well, both which are used to help decide the measures to balance the system [3]. The control board is like the processor in a computer and deals with all the information coming in from the sensors and then talks to the components accordingly to deal with said data. The control board sends out the signals to the motors to activate them accordingly whether it is a command prompt from the user to simply move forward or to rebalance itself after the gyro noticed that it is not in balance. The control board requires a lot of power due to having to process data real time and to have to make micro adjustments in the speed and balance all while ensuring smooth movements to keep the user as comfortable as possible. Another system that many human transporters tend to have is regenerative braking. Given that the transporter uses electric motors, a regenerative braking feature is implemented into many segways like that of electric cars using electric motors.

3 Methodology

There were various outcomes that were required from the project. The first requirement being the system's free body diagrams and kinetic diagrams. The system was simplified and only required one diagram representing the wheel and another diagram representing the handlebar segment of the segway.

The next requirement involves creating a mathematical model for the system. The project provided two equations that specified the form that the equations should take. These equations can be found below:

$$\begin{cases} C_1\ddot{x}(t) + C_2(\theta)\ddot{\theta}(t) + C_3(\theta)\dot{\theta}^2(t) = C_7u(t) \\ C_4\dot{\theta}(t) + C_5(\theta)\ddot{x}(t) + C_6(\theta) = 0 \end{cases}$$

After completing the mathematical model, the transporter was to be modeled in Simulink. The mathematical model was to be expressed in a standard state-variable model and then solved. From there the next task was to adjust the parameters of the transporter to let the transporter travel around five to ten meters. This was to be done by choosing a thrust force and then fine tuning the chosen thrust force to get it to translate for the set amount. This model was then built in SimulationX.

3.1 FBD and KD of the Subsystems

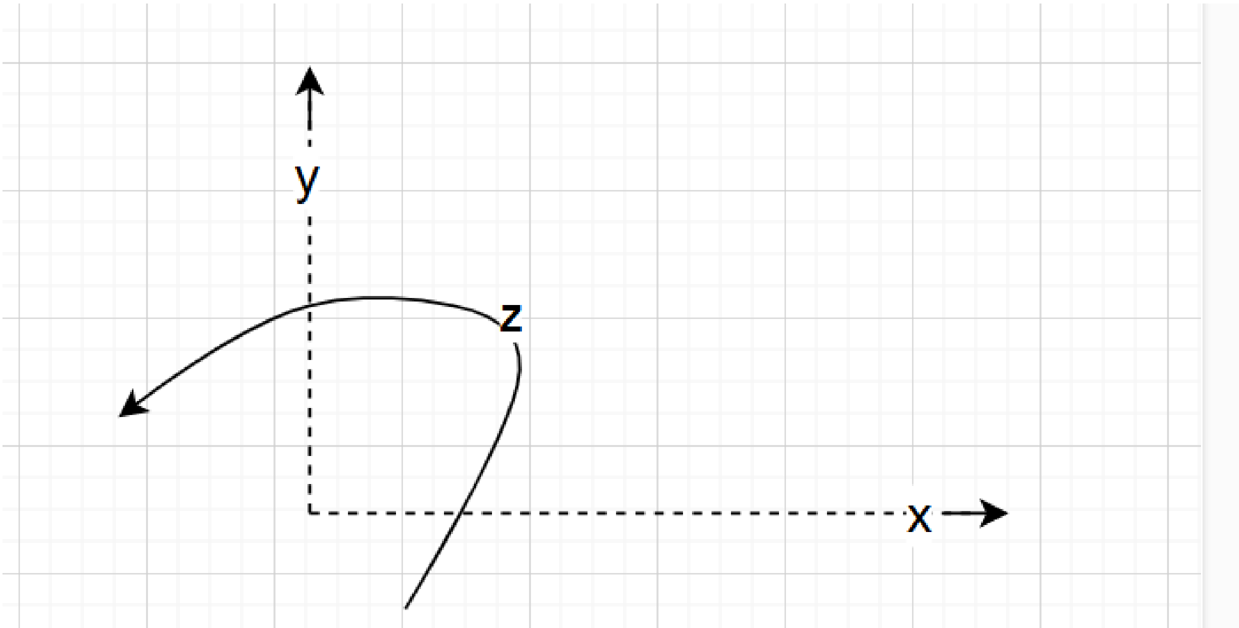

Figure 1: Axis

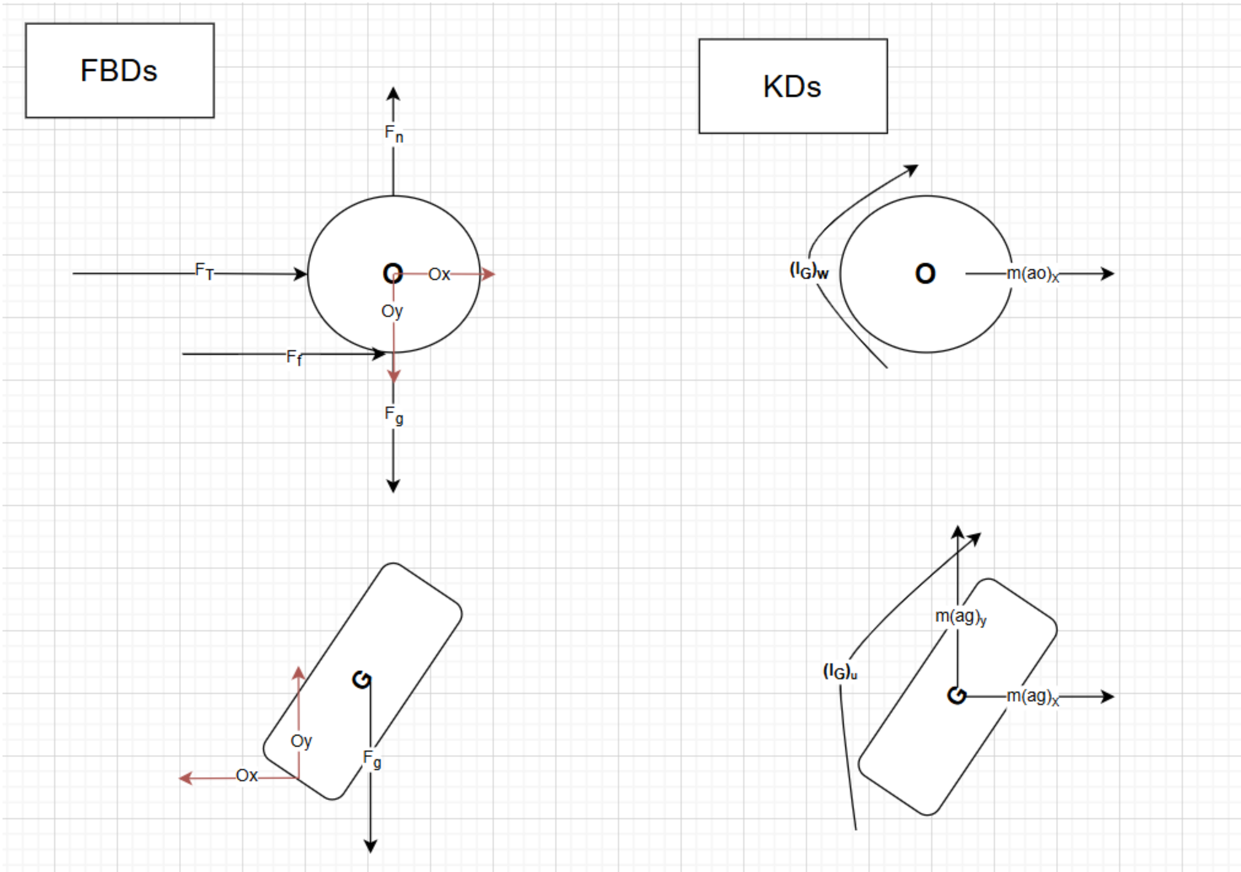

Figure 2: Free Body Diagrams & Kinetic Diagrams

For Wheel-Base Subsystem:

Table 1: Describing the Forces in the Wheel-Base Subsystem

F_n	This is the normal force, and is force of the ground pushing back on the wheel-base.
F_g	This is the force of gravity on the wheel-base subsystem.
F_f	This is the force of friction, and it opposes the assumed direction of motion of the wheel-base subsystem.

F_T	This is the thrust force, and is the input to the system. It is a fixed force, and is generated by the internal torque of the motors. The inertia is ignored in the later calculations, as this force models the motors. Furthermore, this force is located at the middle of the base in-line with the wheel's axle.
O_x	This is the support reaction of the user subsystem on the wheel-base subsystem in the x-direction.
O_y	This is the support reaction of the user subsystem on the wheel-base subsystem in the y-direction.

For User Subsystem:

Table 2: Describing the Forces in the User Subsystem

F_g	This is the force of gravity on the user subsystem.
O_x	This is the support reaction of the wheel-base subsystem on the user subsystem in the x-direction.
O_y	This is the support reaction of the wheel-base subsystem on the user subsystem in the y-direction.

3.2 Mathematical Model of the Transporter

For Pendulum - User Subsystem:

The acceleration of the pendulum-user subsystem was given as:

$$\mathbf{a_G} = \left(\ddot{x}+L_G\cos(\theta+\beta)\ddot{\theta}-L_G\sin(\theta+\beta)\dot{\theta}^2\right)\hat{\mathbf{i}} + \left(-L_G\sin(\theta+\beta)\ddot{\theta}-L_G\cos(\theta+\beta)\dot{\theta}^2\right)\hat{\mathbf{j}}$$

This is in fixed axis rotation around point O, thus the governing equations are:

$$\sum F_x = m(a_G)_x = m\ddot{x}_G$$

$$\sum F_y = m(a_G)_y = m\ddot{y}_G$$

$$\sum M_O = I_O\alpha = I_O\ddot{\theta}$$

$$I_O = I_G + mr_{G/O}^2$$

Applying these equations to the FBDs from section 3.1:

$$\sum F_x = m_u a_{Gx}$$

$$-O_x = m_u\left(\ddot{x}+L_G\cos(\theta+\beta)\ddot{\theta}-L_G\sin(\theta+\beta)\dot{\theta}^2\right)$$

$$-O_x = m_u\left(\ddot{x}+L_G\cos(\theta+\beta)\ddot{\theta}-L_G\sin(\theta+\beta)\dot{\theta}^2\right) \tag{1}$$

And in the y-direction:

$$\sum F_y = m_u a_{Gy}$$

$$O_y - m_u g = m_u\left(-L_G\sin(\theta+\beta)\ddot{\theta}-L_G\cos(\theta+\beta)\dot{\theta}^2\right)$$

$$O_y = m_u\left(-L_G\sin(\theta+\beta)\ddot{\theta}-L_G\cos(\theta+\beta)\dot{\theta}^2+g\right) \tag{2}$$

Finally, the moment around G is taken, this eliminates the force of gravity. The reason for taking the moment at point G over point O, is that we need the O_x and O_y forces to solve the equations for the wheel base subsystem.

$$\sum M_O = I_O\alpha = I_O\ddot{\theta}$$

$$-O_x L_G \cos(\theta+\beta) - O_y L_G \sin(\theta+\beta) = -I_G\ddot{\theta}$$

$$O_x L_G \cos(\theta+\beta) + O_y L_G \sin(\theta+\beta) = I_G\ddot{\theta}$$

Replace O_x, and O_y using equations 2 and 3:

$$-m_u\left(\ddot{x}+L_G\cos(\theta+\beta)\ddot{\theta}-L_G\sin(\theta+\beta)\dot{\theta}^2\right)L_G\cos(\theta+\beta)$$

$$+\,m_u\left(-L_G\sin(\theta+\beta)\ddot{\theta}-L_G\cos(\theta+\beta)\dot{\theta}^2+g\right)L_G\sin(\theta+\beta) = I_G\ddot{\theta}$$

Expanding and rearranging:

$$m_u L_g\cos(\theta+\beta)\ddot{x} - m_u L_g^2\cos^2(\theta+\beta)\ddot{\theta} + m_u L_g\sin(\theta+\beta)\cos(\theta+\beta)\dot{\theta}^2 - m_u L_g^2\sin^2(\theta+\beta)\ddot{\theta} -$$

$$m_u L_g\cos(\theta+\beta)\sin(\theta+\beta)\dot{\theta}^2 + m_u g L_g\sin(\theta+\beta) = I_G\ddot{\theta}$$

$$-m_u L_g\cos(\theta+\beta)\ddot{x} - \left[m_u L_g^2(\cos^2(\theta+\beta)+\sin^2(\theta+\beta))\right]\ddot{\theta} - I_G\ddot{\theta} + m_u g L_g\sin(\theta+\beta) = 0$$

Applying Pythagoras identity:

$$-m_u L_g\cos(\theta+\beta)\ddot{x} - \left(m_u L_g^2+I_G\right)\ddot{\theta} + m_u g L_g\sin(\theta+\beta) = 0$$

Finally, applying small angle identity to get the linearized form:

$$-m_u L_g\ddot{x} - \left(m_u L_g^2+I_G\right)\ddot{\theta} + m_u g L_g(\theta+\beta) = 0$$

For Wheel-Base Subsystem:

This is in rectilinear motion along the x-axis; thus the governing equations are:

$$\sum F_x = m(a_G)_x = m\ddot{x}_G$$

$$\sum F_y = m(a_G)_y = 0$$

$$\sum M_G = 0$$

Applying these equations to the FBDs from section 3.1:

$$\sum F_x = m\ddot{x}$$

$$F_T + O_x + F_S = m\ddot{x}$$

From wheel's no slip condition:

$$r\alpha = \ddot{x}$$

$$\alpha = \frac{\ddot{x}}{r}$$

And in the y-direction:

$$\sum F_y = 0$$

$$F_N - mg - O_y = 0$$

Finally, the moment around point O is taken, this eliminates all forces outside of the friction force, as it is the only force not on the same axis as point O. This results in the force of friction being equal to the moment of inertia.

$$\sum M_o = I_o\alpha$$

$$rF_S = -(I_{G,w})\alpha$$

Replacing α, with the no-slip condition.

$$rF_S = -(I_{G,w})\frac{\ddot{x}}{r}$$

$$F_S = -\frac{(I_{G,w})\ddot{x}}{r^2} \tag{3}$$

Next, we subbed equation 3 back into the $\sum F_x$ equation for F_S, and subbed in O_x from equation 1, resulting in this:

$$F_T - m_u\left(\ddot{x}+L_G\cos(\theta+\beta)\ddot{\theta}-L_G\sin(\theta+\beta)\dot{\theta}^2\right) - \frac{(I_{G,w})\ddot{x}}{r^2} = m\ddot{x}$$

$$F_T - m_u\ddot{x} - m_uL_G\cos(\theta+\beta)\ddot{\theta} + m_uL_G\sin(\theta+\beta)\dot{\theta}^2 - \frac{(I_{G,w})\ddot{x}}{r^2} = m\ddot{x}$$

$$F_T = m_u\ddot{x} + m_uL_G\cos(\theta+\beta)\,\ddot{\theta} - m_uL_G\sin(\theta+\beta)\,\dot{\theta}^2 + \frac{(I_{G,w})\ddot{x}}{r^2} + m\ddot{x}$$

This results in the equation being:

$$F_T = \left(m+m_u+\frac{I_{G\omega}}{r^2}\right)\ddot{x} + m_uL_G\cos(\theta+\beta)\ddot{\theta} - m_uL_G\sin(\theta+\beta)\dot{\theta}^2$$

This equation can be simplified using the small identity as mentioned in the project description, thus eliminating the $\dot{\theta}^2$, as it can be approximated as zero. Therefore, the final linearized equation is:

$$F_T = \left(m+m_u+\frac{I_{G\omega}}{r^2}\right)\ddot{x} + m_uL_G\ddot{\theta}$$

Derivation of State Space Equations

Linearize with the small angle approximation:

$$(m + m_u + \frac{I_{G\omega}}{r^2})\ddot{x} + m_uL_G\ddot{\theta} - m_uL_G(x+\beta)\dot{\theta}^2 = F_T$$

Due to the small angle approximation the $m_uL_G(x+\beta)\dot{\theta}^2$ becomes 0

$$-m_uL_G\ddot{x} - (m_uL_G^2 + I_{Gv})\ddot{\theta} + m_ugL_G(\theta + \beta) = 0$$

Inputs: F_T

Outputs: $\theta(t)$, $\mathrm{x}(t)$

$$\begin{cases} x_1(t) = \theta(t) \\ x_2(t) = \dot{x}_1(t) = \dot{\theta}(t) \\ x_3(t) = x(t) \\ x_4(t) = \dot{x}_3(t) = \dot{x}(t) \end{cases}$$

Defined Variables:

$$\begin{bmatrix} \dot{x}_1(t) \\ \dot{x}_2(t) \\ \dot{x}_3(t) \\ \dot{x}_4(t) \end{bmatrix} = \begin{bmatrix} x_2(t) \\ ? \\ x_4(t) \\ ? \end{bmatrix}$$

Starting Equations:

$$\ddot{\theta} = \left[\frac{F_T - \left(m + m_u + \frac{I_w}{r^2}\right)\ddot{x}}{m_u L_G}\right]$$

$$\ddot{x} = \frac{-(m_u L_G^2 + I_v)\ddot{\theta} + m_u g L_h(\theta + \beta)}{m_u L_G}$$

Constants:

$$C_1 = \left(m + m_u + \frac{I_w}{r^2}\right)$$

$$C_2 = m_u L_G, C_3 = 0, C_7 = 1$$

$$C_4 = -(m_u L_G^2 + I_v), C_5 = -m_u L_G$$

$$C_6 = m_u g L_h(\theta + \beta)$$

Solving for theta double dot

$$\ddot{\theta} = \frac{F_T}{m_u L_G} - \frac{(m + m_u + \frac{I_w}{r^2})\ddot{x}}{m_u L_G}$$

$$\ddot{\theta} = \frac{F_T}{m_u L_G} - \frac{(m + m_u + \frac{I_w}{r^2})}{m_u L_G}\left[\frac{-(m_u L_G^2 + I_v)\ddot{\theta} + m_u g L_h(\theta + \beta)}{m_u L_G}\right]$$

$$\ddot{\theta} = \frac{F_T}{m_u L_G} - \left[\frac{-(m + m_u + \frac{I_w}{r^2})(m_u L_G^2 + I_v)\ddot{\theta} + (m + m_u + \frac{I_w}{r^2})m_u g L_h(\theta + \beta)}{(m_u L_G)^2}\right]$$

$$\ddot{\theta} = \frac{F_T}{m_u L_G} + \left[\frac{(m + m_u + \frac{I_w}{r^2})(m_u L_G^2 + I_v)\ddot{\theta} - (m + m_u + \frac{I_w}{r^2})m_u g L_h(\theta + \beta)}{(m_u L_G)^2}\right]$$

$$\ddot{\theta} = \frac{F_T}{m_u L_G} + \frac{(m + m_u + \frac{I_w}{r^2})(m_u L_G^2 + I_v)\ddot{\theta} - (m + m_u + \frac{I_w}{r^2})m_u g L_h(\theta + \beta)}{(m_u L_G)^2}$$

$$\ddot{\theta}\left(1 - \frac{(m + m_u + \frac{I_w}{r^2})(m_u L_G^2 + I_v)}{(m_u L_G)^2}\right) = \frac{F_T}{m_u L_G} - \frac{(m + m_u + \frac{I_w}{r^2})m_u g L_h(\theta + \beta)}{(m_u L_G)^2}$$

$$\ddot{\theta}\left(1 + \frac{C_1(C_4)}{C_2^2}\right) = \frac{F_T}{C_2} - \frac{C_1 C_2 g(\theta + \beta)}{C_2^2}$$

$$\ddot{\theta}\left(1 + \frac{C_1(C_4)}{C_2^2}\right) = \frac{F_T}{C_2} - \frac{C_1 g\theta}{C_2} - \frac{C_1 g\beta}{C_2}$$

$$\ddot{\theta} = \frac{F_T/C_2 - \frac{C_1 g\theta}{C_2} - \frac{C_1 g\beta}{C_2}}{\left(1 + \frac{C_1(C_4)}{C_2^2}\right)}$$

$$\ddot{\theta} = \frac{F_T}{C_2 + \frac{C_1 C_4}{C_2}} - \frac{C_1 g\theta}{C_2 + \frac{C_1 C_4}{C_2}} - \frac{C_1 g\beta}{C_2 + \frac{C_1 C_4}{C_2}}$$

Subbing in Constants into x double dot

$$\ddot{x} = \frac{C_4\ddot{\theta} + C_2 g(\theta + \beta)}{C_2}$$

$$\ddot{x} = \frac{C_4}{C_2}\ddot{\theta} + g(\theta + \beta)$$

Subbing in the $\ddot{\theta}$ equation into the x double dot equation

$$\ddot{\theta} = \frac{F_T}{C_2 + \frac{C_1 C_4}{C_2}} - \frac{C_1 g\theta}{C_2 + \frac{C_1 C_4}{C_2}} - \frac{C_1 g\beta}{C_2 + \frac{C_1 C_4}{C_2}}$$

$$\ddot{x} = \frac{C_4}{C_2}\left(\frac{F_T}{C_2 + \frac{C_1 C_4}{C_2}} - \frac{C_1 g\theta}{C_2 + \frac{C_1 C_4}{C_2}} - \frac{C_1 g\beta}{C_2 + \frac{C_1 C_4}{C_2}}\right) + g(\theta + \beta)$$

$$\ddot{x} = \frac{C_4 F_T}{C_2^2 + C_1 C_4} - \frac{C_1 C_4 g\theta}{C_2^2 + C_1 C_4} - \frac{C_1 C_4 g\beta}{C_2^2 + C_1 C_4} + g\theta + g\beta$$

Group terms together

$$\ddot{x} = \left(\frac{C_4}{C_2^2 + C_1 C_4}\right) F_T + \left(-\frac{C_1 C_4 g}{C_2^2 + C_1 C_4} + g\right)\theta + \left(-\frac{C_1 C_4 g}{C_2^2 + C_1 C_4} + g\right)\beta$$

Final Matrix

$$\begin{bmatrix} \dot{x}_1(t) \\ \dot{x}_2(t) \\ \dot{x}_3(t) \\ \dot{x}_4(t) \end{bmatrix} = \begin{bmatrix} 0 & 1 & 0 & 0 \\ -\dfrac{C_1 g}{C_2 + \dfrac{C_1 C_4}{C_2}} & 0 & 0 & 0 \\ 0 & 0 & 0 & 1 \\ -\dfrac{C_1 C_4 g}{C_2^2 + C_1 C_4} + g & 0 & 0 & 0 \end{bmatrix} \begin{bmatrix} x_1(t) \\ x_2(t) \\ x_3(t) \\ x_4(t) \end{bmatrix} + \begin{bmatrix} 0 \\ -\dfrac{C_1 g}{C_2 + \dfrac{C_1 C_4}{C_2}} \\ 0 \\ -\dfrac{C_1 C_4 g}{C_2^2 + C_1 C_4} + g \end{bmatrix} \beta + \begin{bmatrix} 0 \\ \dfrac{1}{C_2 + \dfrac{C_1 C_4}{C_2}} \\ 0 \\ \dfrac{C_4}{C_2^2 + C_1 C_4} \end{bmatrix} F(t)$$

3.3 Tuning the Thrust Force

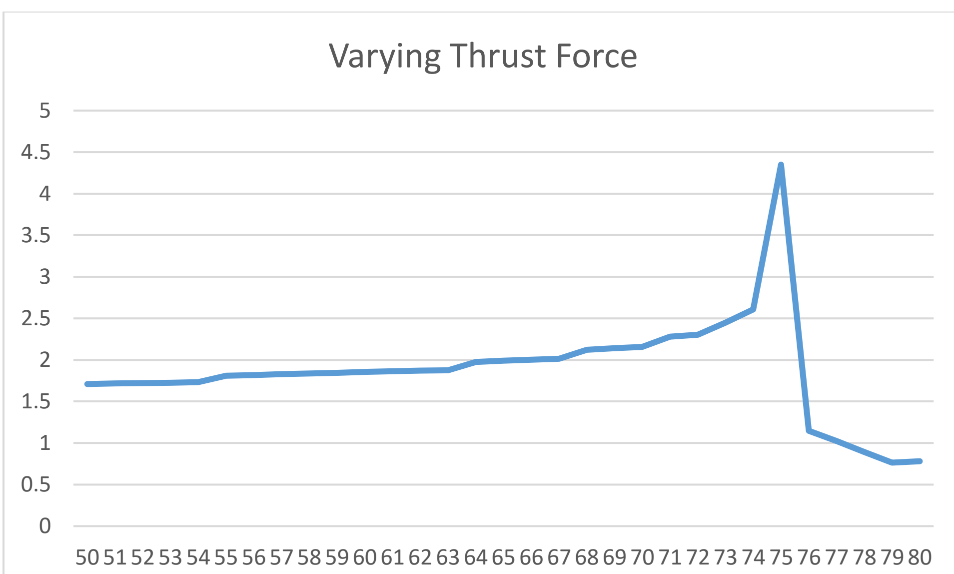

Figure 3: Variation of Thrust Force

To tune the thrust force, the alpha and beta angles were kept constant and at their original values of five degrees. From there the thrust force was varied between the values of 50 and 80 Newtons. As seen in Figure 3, there is a significant increase in the displacement at a thrust force of 75 N, and as such it was selected as the thrust force for the project.

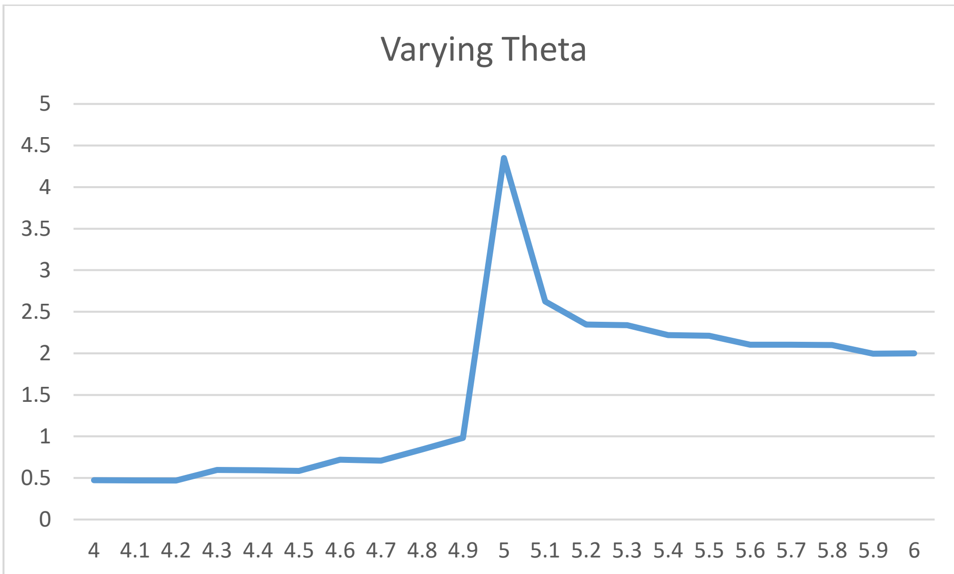

Figure 4: Variation of Theta Graph

After the selection of the thrust force, a similar process was done to select the theta value. The Thrust force was kept constant at the chosen value and beta was constant at the base value of 5 degrees while theta was being varied. Theta seemed to provide the largest displacement when it was at a value of 5 degrees so it that was the selected angle.

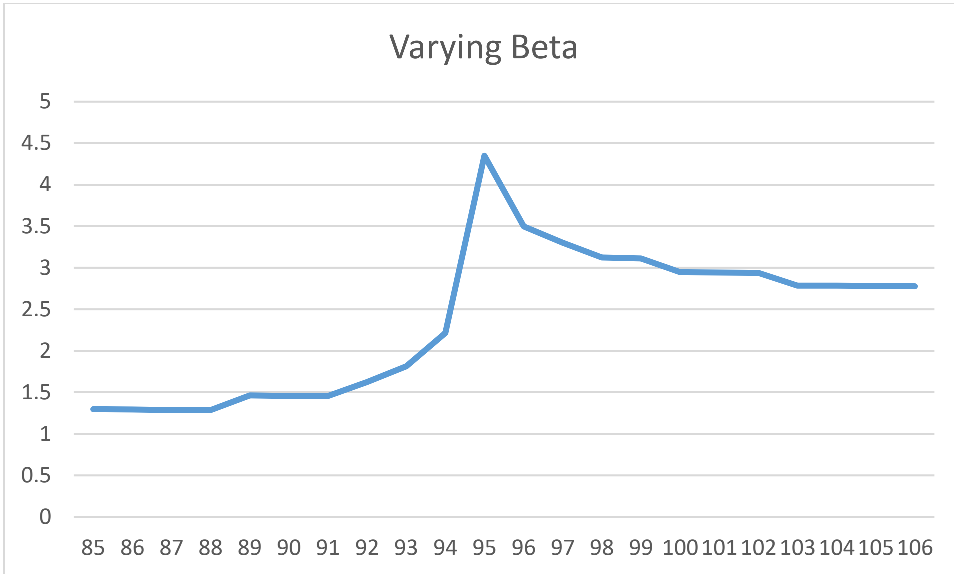

Figure 5: Variation of Beta Graph

Finally for beta, the theta and thrust force values were finalized while beta was being varied. The beta value that provided the largest displacement was 95 degrees, or 5 additional degrees of tilt for the handlebar.

Finally, the thrust force was manually tuned to a value of 75.014N, using the previously defined theta and beta values. This manual process consisted of repeatedly trying values between 75 and 76 meters to result in the largest displacement possible. Overall, the process taken was quite simple and simply involved maximizing one of the three variables at a time and trying to increase the displacement with each successive variable.

3.4 Modelling & Testing the SimulationX

The process for modelling the SimulationX, was to base it around existing segways such as the one included in the figure below. However, it is essential to consider the specific dimensions given and modify the model to best suit them. The final selected dimensions can be seen in the results section.

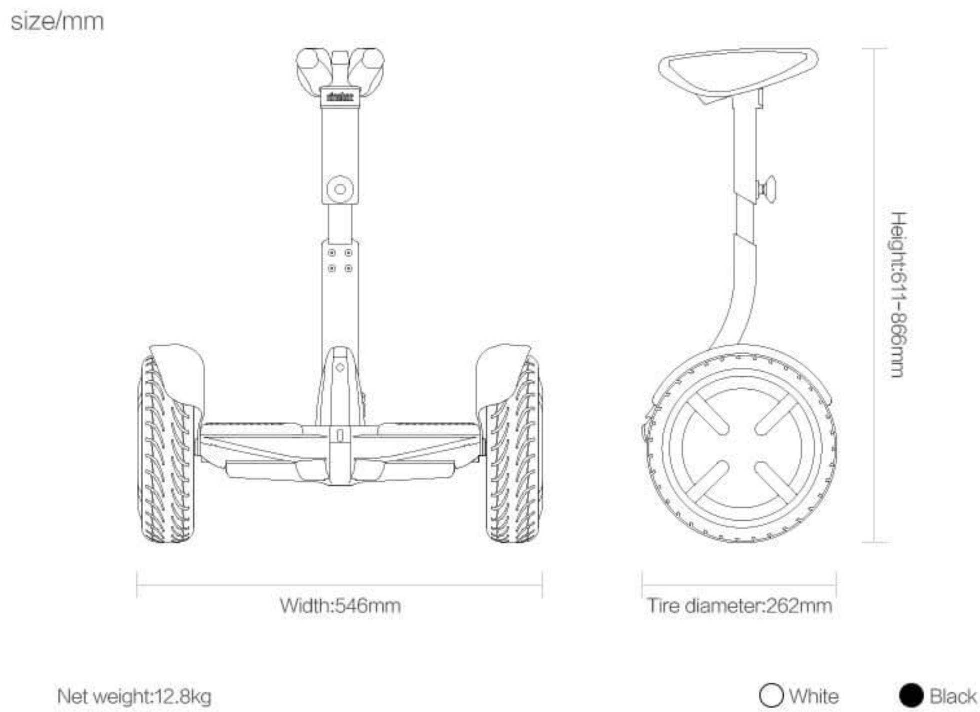

Figure 6: Segway Diagram [4]

In the figure above, the distance between the ends of each wheel was 546mm or 54.6 cm, thus the distances between the center of each wheel were selected to be a similar value of 50cm apart. Furthermore, as the wheel radius was provided to be 12.7 cm, the width of the wheel was selected to the same to maintain consistency, and simplify the modelling process. The axles were modelled with a revolute joint for each wheel. This allowed rotation only in the y-direction. Finally, two prismatic joints were used, the first was used to allow displacement along the x-axis, or the road, and the second to allow rotation in the z-axis.

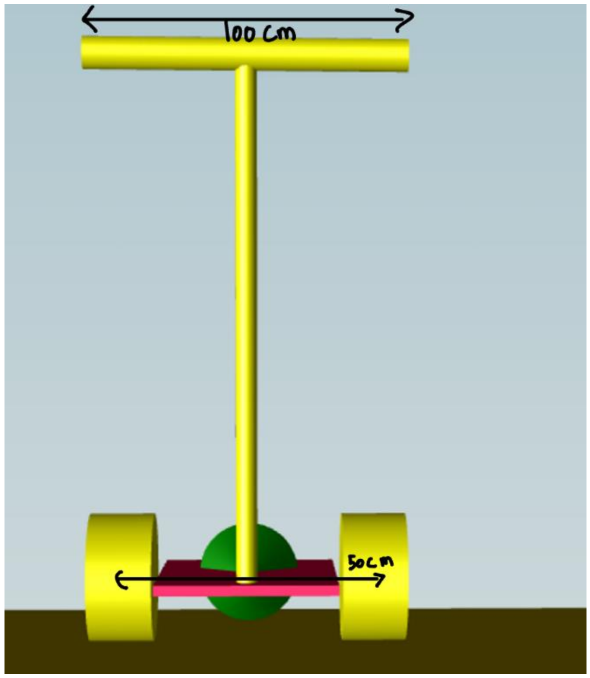

Figure 7: Model of the Handlebar

The base was built to rest in between the wheels. As the wheels were 50cm apart from their centers, and the width of the wheels is 12.7cm, meaning the base should have an x-length of 50 – 12.7/2 – 12.7/2 or 37.3cm. The y-length was selected to 50cm to allow for sufficient room for humans' feet. Lastly, the z-direction was selected to be 2cm. A thinner base was chosen to prevent clipping of the ground as the segway moves over various surfaces.

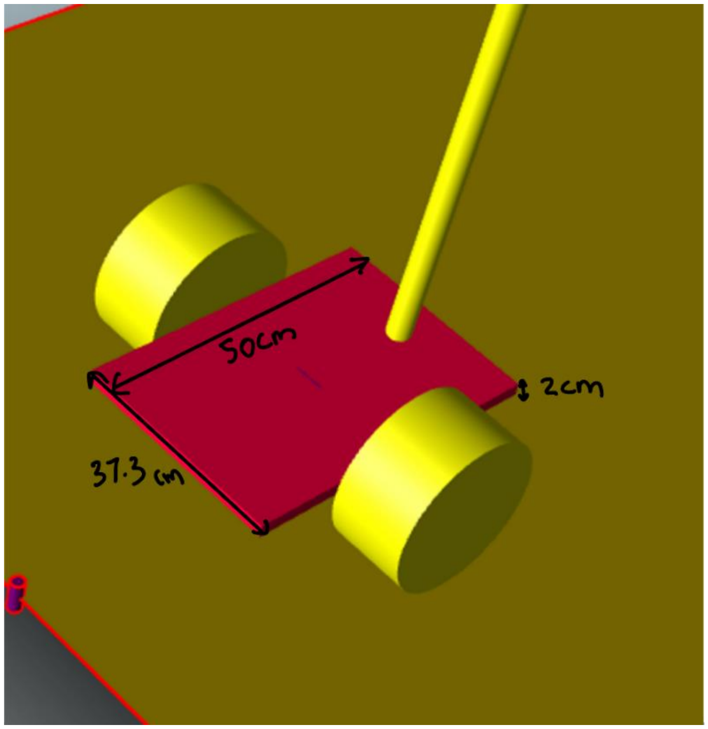

Figure 8: Model of the Base

Next, the handlebar was modelled. The length of the handlebar was given to be 1m, or 100cm. The width of the handlebar was selected to be 74.6 cm, this was on the basis that the handlebar is double the base. This consistency between dimensions will make the design more aesthetically appealing. To add, the radius of the handlebar was selected to be 3cm. This was due to similar applications having similar radii. For example, bicycle handlebars are generally between 3 and 4cm, likewise with hammers and other tools. This will allow for a comfortable segway experience.

4 Results and discussion

4.1 Task 1 Results

System FBD	System KD

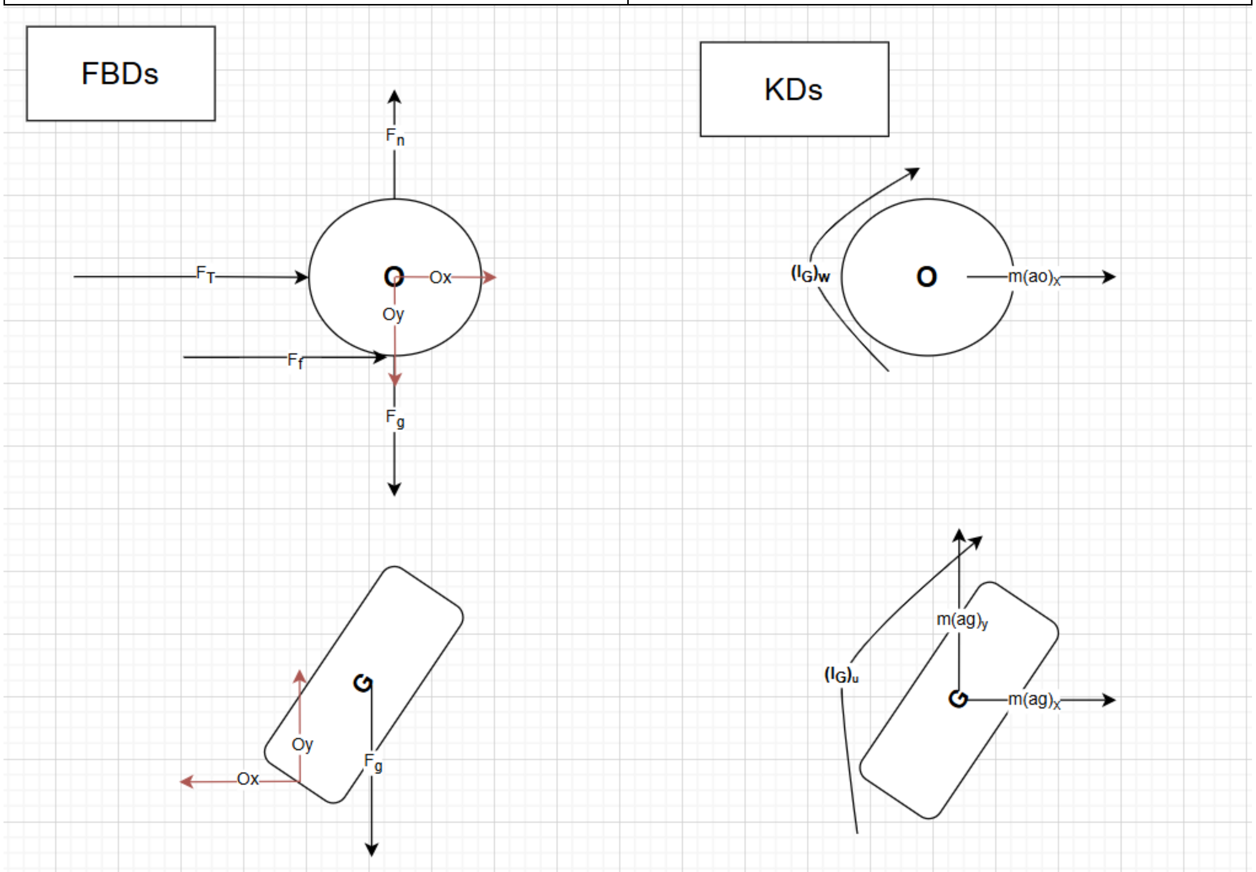

4.2 Task 2 Results

Final Analytical Equations	$(m + m_u + \frac{I_{G\omega}}{r^2})\ddot{x} + m_u L_G \ddot{\theta} - m_u L_G (x+\beta)\dot{\theta}^2$ $= F_T$ $-m_u L_G \ddot{x} - (m_u L_G^2 + I_{Gv})\ddot{\theta} + m_u g L_G (\theta \ + \beta)$ $= 0$

4.3 Task 3 Results

Final Linearized Equation 1	$F_T = \left(m+m_u+\frac{I_{G\omega}}{r^2}\right)\ddot{x} + m_u L_G \ddot{\theta}$
Final Linearized Equation 2	$-m_u L_g \ddot{x} - \left(m_u L_g^2+I_G\right)\ddot{\theta} + m_u g L_g(\theta+\beta) = 0$
Final Standard State Variable Form	

$$\begin{bmatrix} \dot{x}_1(t) \\ \dot{x}_2(t) \\ \dot{x}_3(t) \\ \dot{x}_4(t) \end{bmatrix} = \begin{bmatrix} 0 & 1 & 0 & 0 \\ -\dfrac{C_1 g}{C_2 + \frac{C_1 C_4}{C_2}} & 0 & 0 & 0 \\ 0 & 0 & 0 & 1 \\ -\dfrac{C_1 C_4 g}{C_2^2 + C_1 C_4} + g & 0 & 0 & 0 \end{bmatrix} \begin{bmatrix} x_1(t) \\ x_2(t) \\ x_3(t) \\ x_4(t) \end{bmatrix} + \begin{bmatrix} 0 \\ -\dfrac{C_1 g}{C_2 + \frac{C_1 C_4}{C_2}} \\ 0 \\ -\dfrac{C_1 C_4 g}{C_2^2 + C_1 C_4} + g \end{bmatrix} \beta + \begin{bmatrix} 0 \\ \dfrac{1}{C_2 + \frac{C_1 C_4}{C_2}} \\ 0 \\ \dfrac{C_4}{C_2^2 + C_1 C_4} \end{bmatrix} F(t)$$

4.4 Task 4 Results

M_u	61.5kg
F_T	25 N
Beta	-0.1 radians (-5.7 degrees)
Theta	0.1 radians (5.7 degrees)

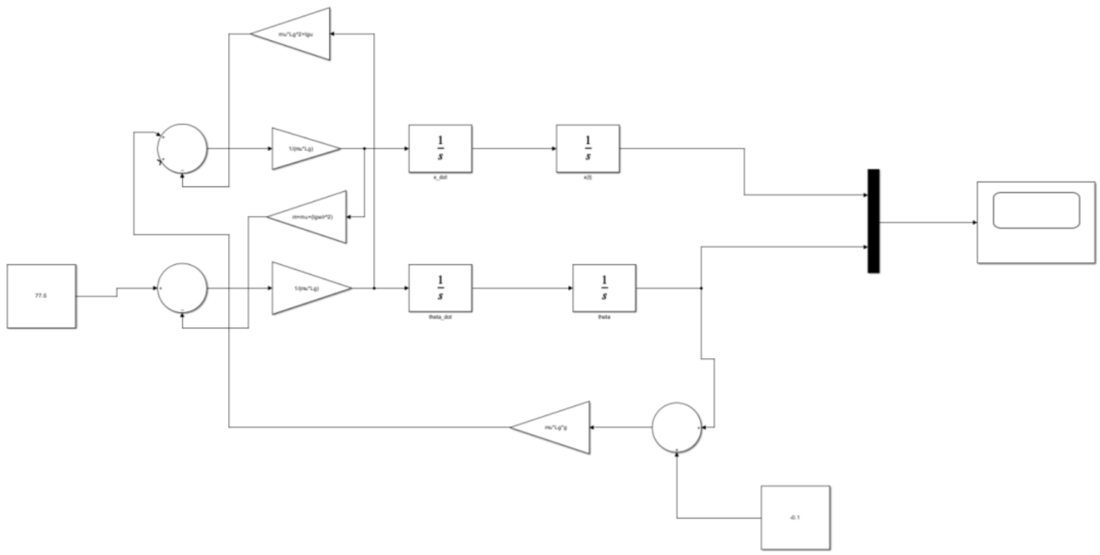

Figure 9: Simulink Model

Initial Observations?

With these initial values, the segway in Simulink was able to travel for approximately 1.2 meters. The other key observations include the exponential behavior of both the position of the segway, in yellow, and the angle of the user in blue. Both graphs have similar behavior, except for their directions being opposite.

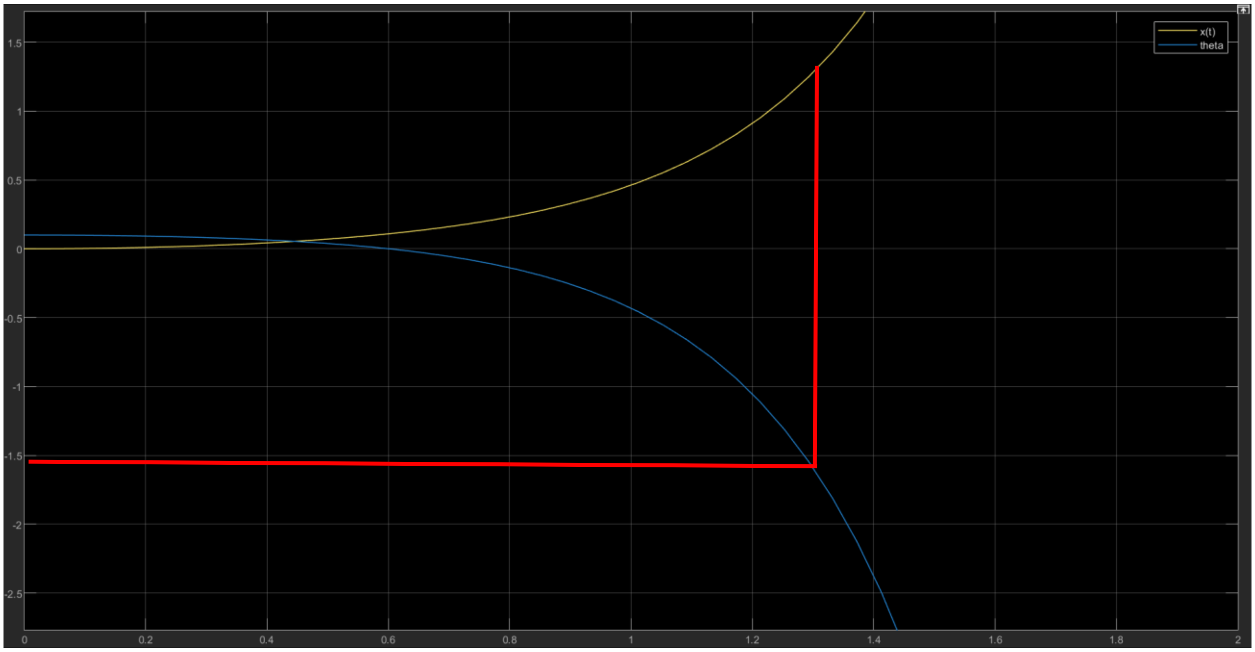

Figure 10: x(t) and theta graphs

4.5 Task 5 Results

Final Thrust Force	77.5 N

Does thrust force have any effect?

After tuning the thrust force, the effect was not as significant as initially anticipated, with a force of 77.5N providing the longest displacement of ~1.6m, as seen in Figure 11.

Does the mass of the base have any effect?

The mass of the base has a significant effect on the behavior of the segway. Initially, with a mass of 35kg, the segway is able to travel approximately 1.6m in about a second before falling. Similarly, a base mass of 10kg results in a similar distance travelled, however it falls before a second. Lastly, the 60 kg base mass decreases the distance travelled to 1.2m, but take the longest time to fall, with approximately 1.2 seconds. This is expected behavior as a lighter system should travel faster than a heavier one. The

Simulink plots for the referenced values can be seen below, the red lines are used to indicate when the user has fallen, this is when 90 degrees has been reached, or ~1.57 radians.

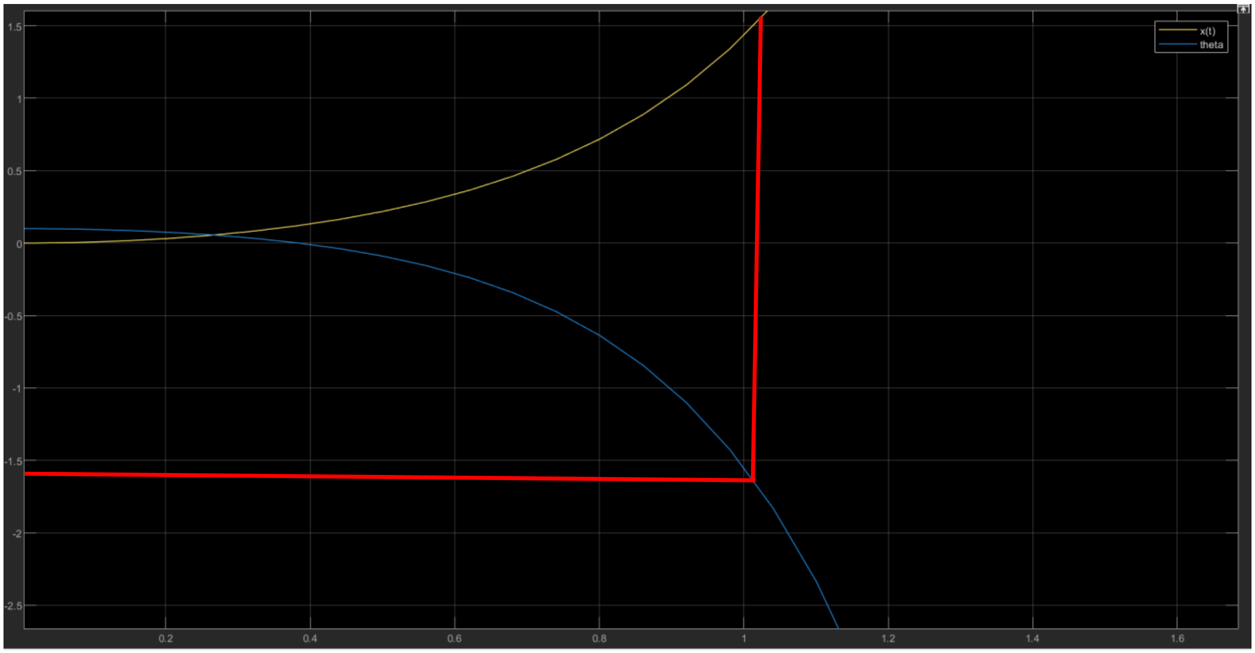

Figure 11: x(t) vs theta for 35kg base mass achieving 1.5m

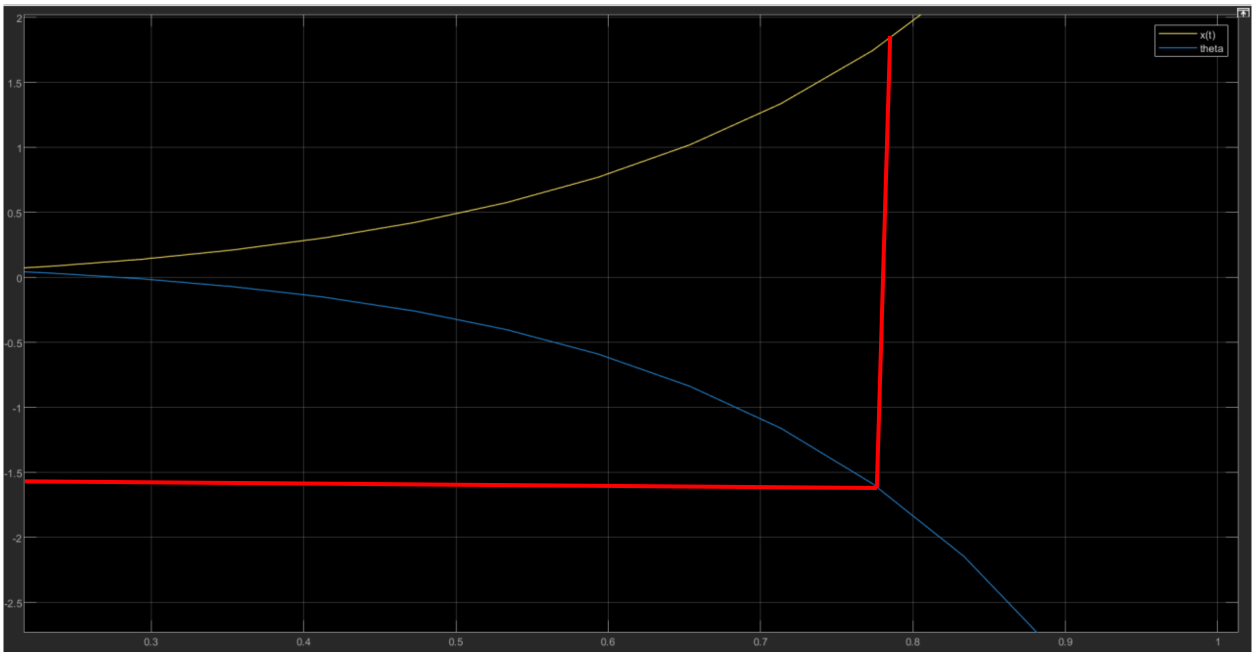

Figure 12: x(t) vs theta for 10kg base mass achieving 1.5m

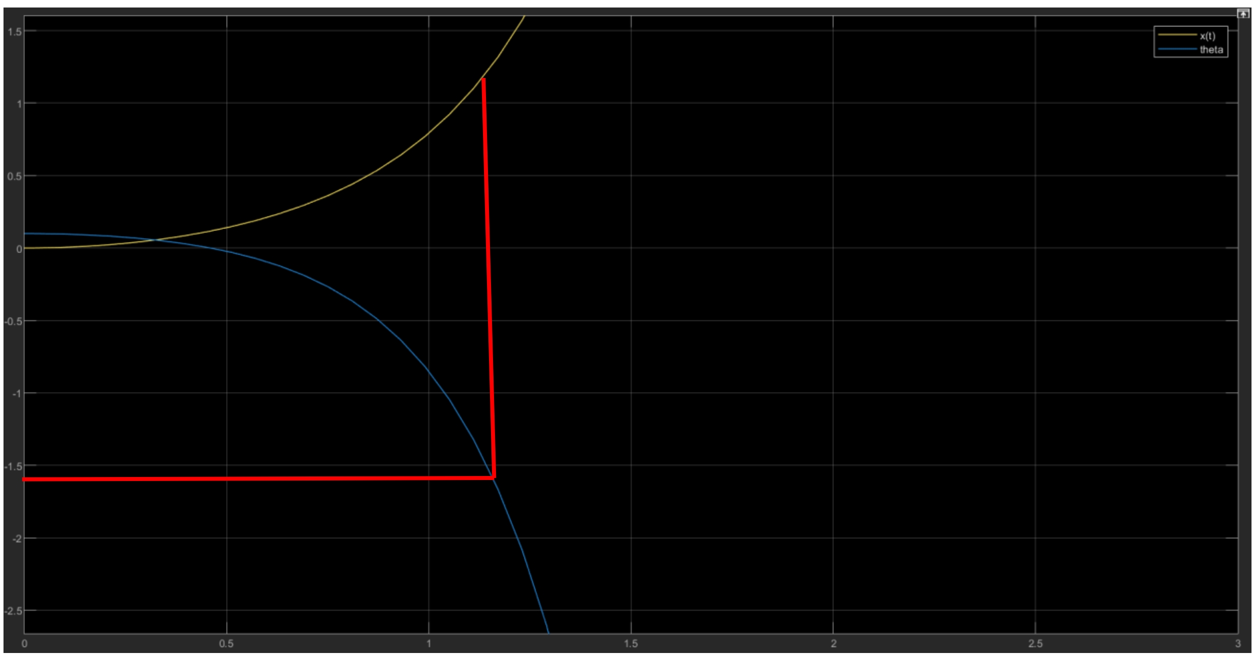

Figure 13: x(t) vs theta for 60kg base mass achieving 1.1m

4.6 Task 6 Results

Table 3: Task 6 Results for Wheel

Wheel Radius (GIVEN)	12.7 cm
Distance between wheel centers	50 cm
Mass of wheel	1 kg

Table 4: Task 6 Results for Base

Base X Dimension	50 cm
Base Y Dimension	37.3 cm
Base Z Dimension	2 cm
Mass of Base	5 kg

Table 5:Task 6 Results for Handlebar

Length of handlebar (GIVEN)	100 cm
Radius of handlebar	2 cm
Width of Handlebar	74.6 cm

4.7 Task 7 Results

Table 6: Task 7 Results for Head

Head X Dimension	Head Y Dimension	Head Z Dimension
12.7 cm (5 in)	12.7 cm (5 in)	12.7 cm (5 in)

Table 7: Task 7 Results for Body

Body X Dimension	Body Y Dimension	Body Z Dimension
12.7cm (5 in)	35cm	76.2cm (30 in)

Table 8: Task 7 Results for Legs

Leg X Dimension	Leg Y Dimension	Leg Z Dimension
5 in	5 in	30 in

4.8 Task 8 Results

Table 9: Task 8 Results

M_u	61.5kg
F_T	50 N
Beta	5 degrees

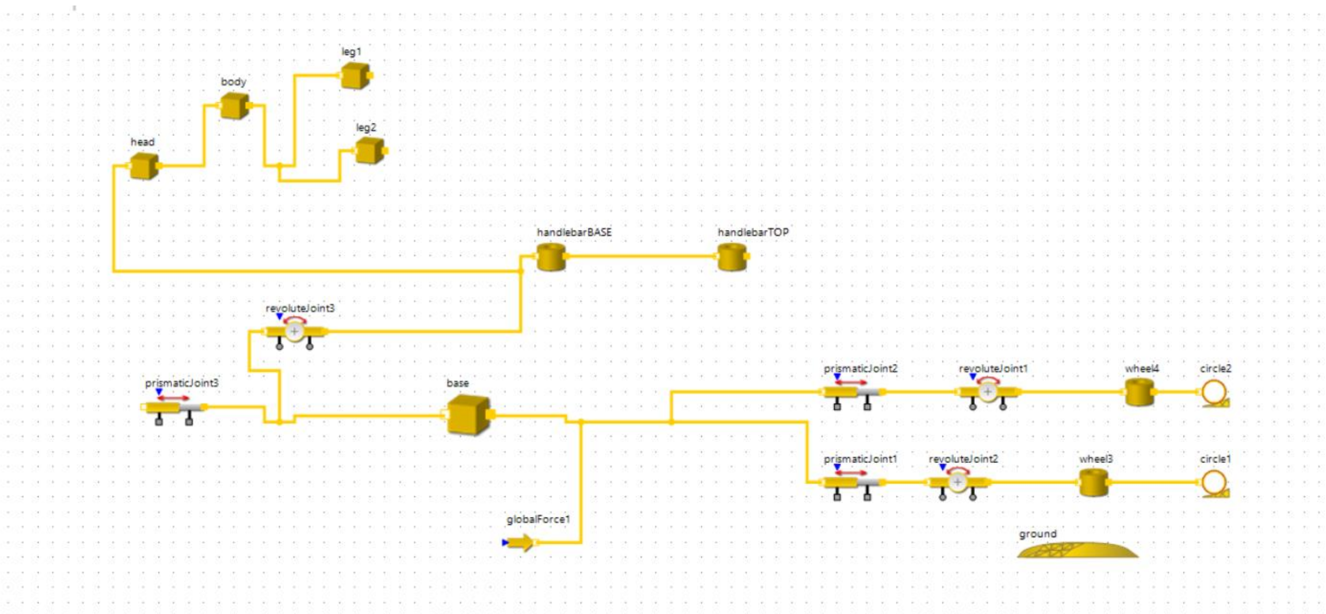

Figure 14: SimulationX Model

F_T	50 N

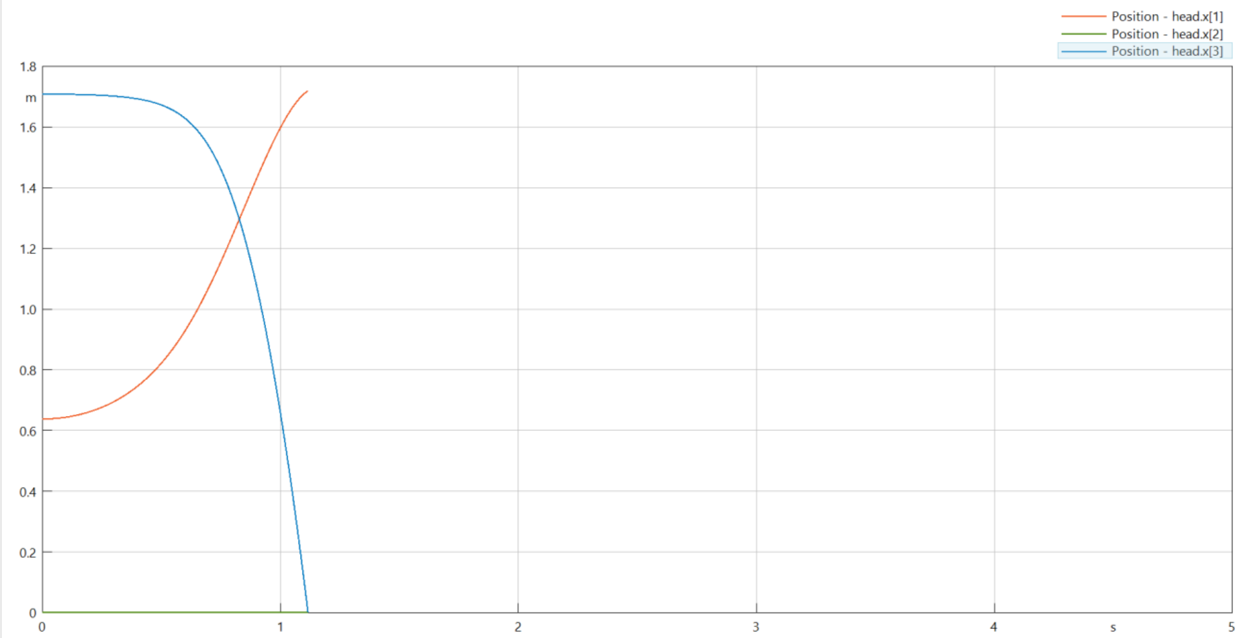

Figure 15: Position with Thrust Force = 50 N, ~1.7m

F_T	60 N

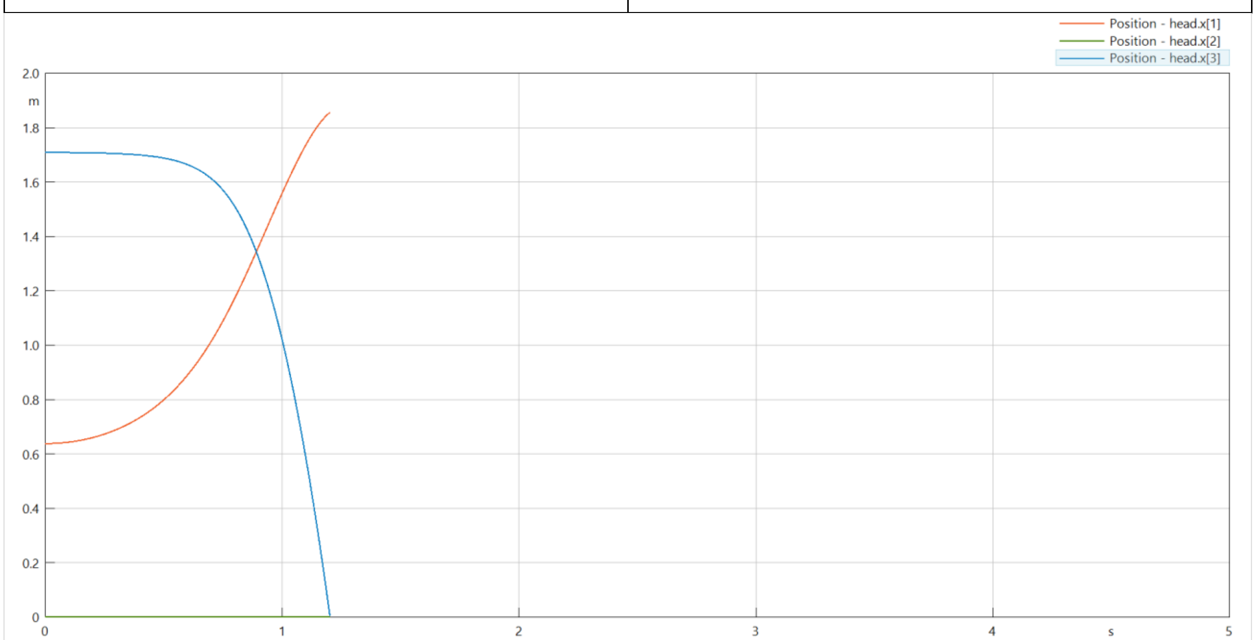

Figure 16: Position with Thrust Force = 60 N, ~1.85m

F_T	70 N

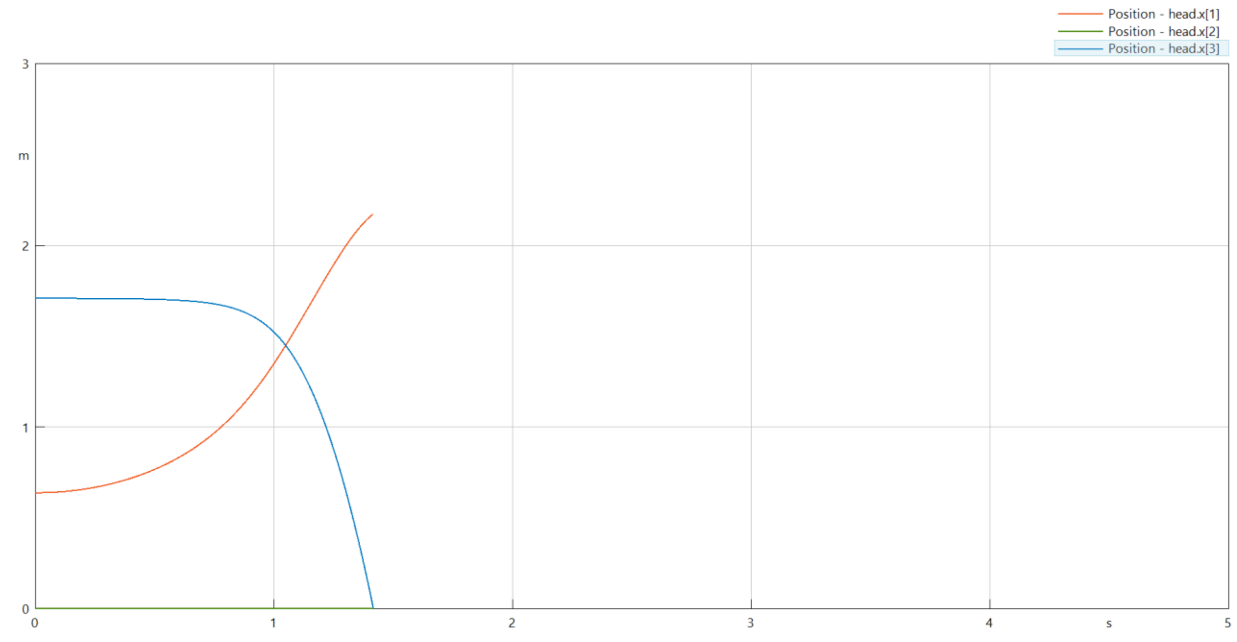

Figure 17: Position with Thrust Force = 70 N, ~2.25m

F_T	80 N

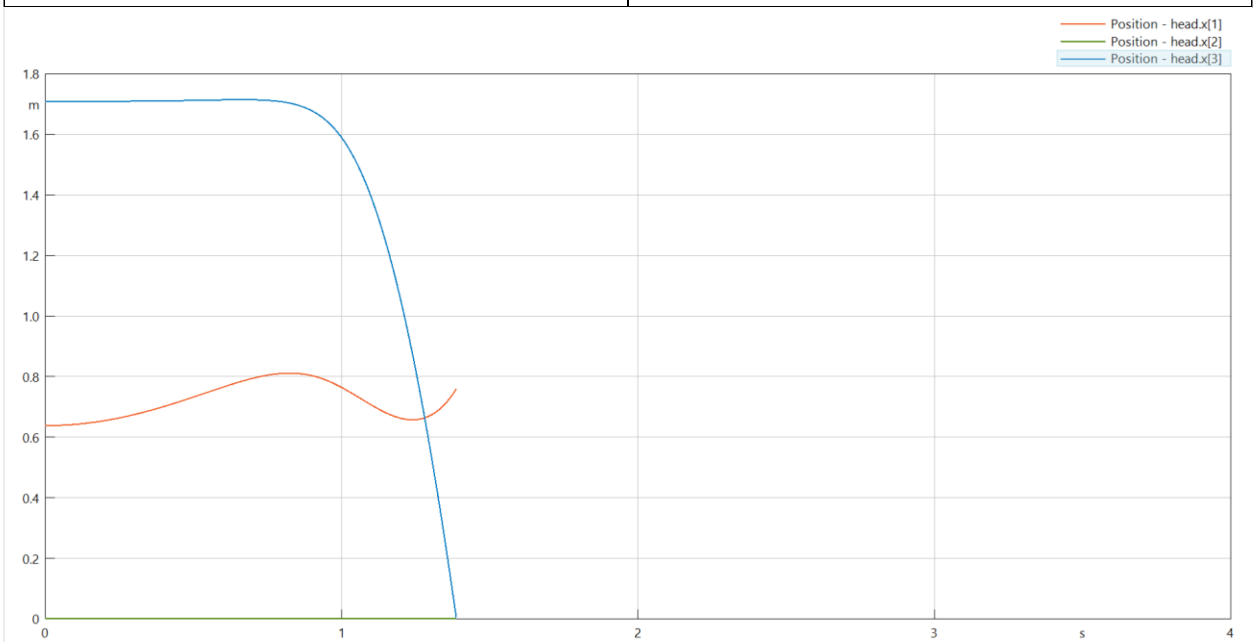

Figure 18: Position with Thrust Force = 80 N, ~0.8m

Initial Observations?

After attempting various thrust forces, it was interesting to see a 3D visual of the segway in motion. To add, it was observed that a thrust force of 70N was the only one to move the segway past 2m. Furthermore, any thrust force more than 80N resulted in the user falling backwards instead of forwards. This decisive force value indicated that a force these large pushes the segway from under the user resulting in the user falling backwards. With this information, the thrust force was tuned further in the range of 70-80 N, with the objective of the user moving the farthest and falling forwards.

4.9 Task 9 Results

Final F_T	75.014 N

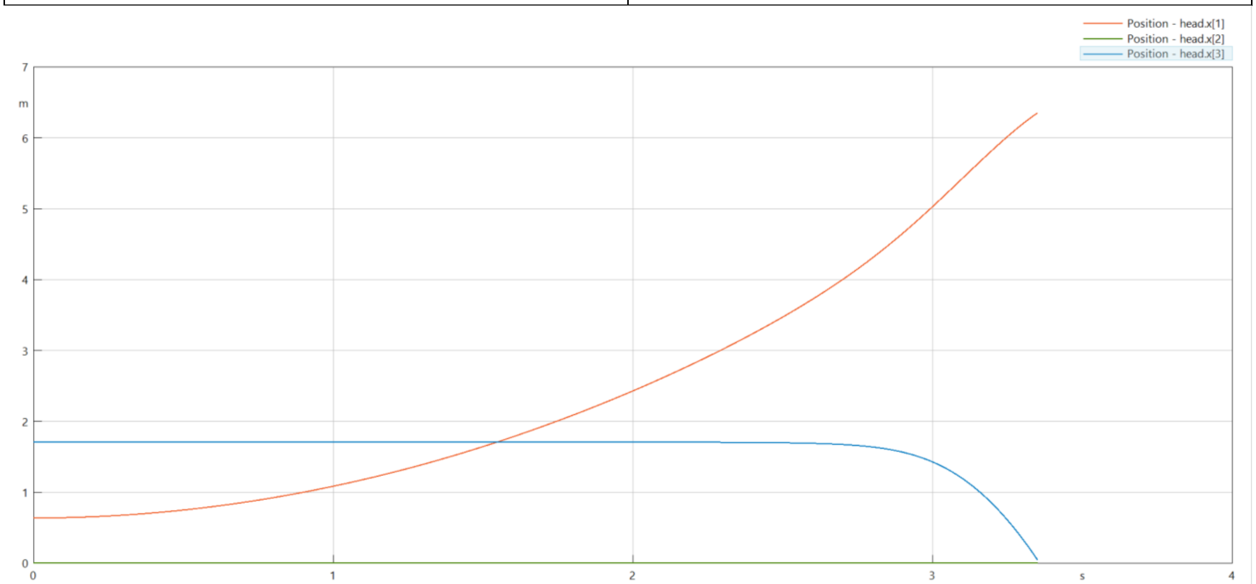

Figure 19: Position with Thrust Force = 75.014 N

4.10 Task 10 Results

Comparing the F_t for both the experimental and numerical model shows us that the best F_t worked similarly in both models. In the numerical model, a thrust force of 77.5N allowed the segway to travel the farthest without falling, while in the experimental model, a similar result was observed at 75.014N. In both cases, forces below this range resulted in limited movement, and forces above caused the user to fall backward. It was observed that the F_t value was most optimal between 70-80N in both models. However, the distance travelled was significantly different in both, with the SimulationX, tripling the distance of the Simulink. To keep the transporter upright the entire time without falling, we would recommend integrating a PID controller into the Simulink model which could adjust the thrust force based on the user's tilt angle (theta). This would allow the segway to respond dynamically and correct itself when tipping begins.

5 Conclusions and recommendations (1-2 pages)

The results from the analysis provide important insights into the performance and stability of the self-balancing transporter system, highlighting key factors that influence its behavior under various conditions. In particular, the experimental (SimulationX) and numerical (Simulink) models both contribute to a clearer understanding of the system's thrust force requirements and its interaction with the base's mass.

The experimental model demonstrated that a thrust force of 75.014N was optimal for maintaining forward motion without the user falling backward. The numerical models, however, suggested a slightly higher thrust force of 77.5 N. Additionally, the mass of the base was shown to display a significant role in the system's overall performance. Heavier bases were observed to reduce travel distance, this is likely due to the increased inertia, which requires more force for the same amount of motion. However, these heavier bases also change the time taken before the tipping of the user, suggesting that while additional weight can improve stability by resisting tipping forces, it comes at the cost of speed and responsiveness. Therefore, balancing the mass of the base is crucial, as it impacts both the range of travel and the tipping conditions. Another key takeaway from our results is that small variations in applied thrust have a significant effect on stability. In particular, exceeding 80 N resulted in instability and the user falling backward, indicating that there is a tradeoff between propulsion and user positioning. To improve control and reliability, a key recommendation is to implement an adaptive thrust control system that dynamically adjusts force based on user movement and tilt angle, ensuring smoother acceleration without destabilization.

From a design perspective, reducing the weight of the base while maintaining structural integrity would improve responsiveness. A lighter base would allow quicker turns and more efficient use of thrust. A composite material with high strength-to-weight ratio could be used to optimize performance, while also reducing the overall mass of the system.

In conclusion, the analysis of this project shows that the balance between thrust force, base weight, and stability is critical for the self-balancing transporter's performance. By fine-tuning these parameters and adding a system that adjusts thrust based on real-time feedback, the transporter can be made more stable and responsive. Future improvements should focus on making the system more efficient by reducing the weight of the base and improving how the thrust is controlled, ensuring a smoother and more reliable ride for the user.

6 References

[1] “How do segways, hoverboards and other self-balancing personal transporters work?,” How self-balancing personal transporters work? | Planète Énergies, https://www.planete-energies.com/en/media/article/how-do-segways-hoverboards-and-other-self-balancing-personal-transporters-work (accessed Apr. 3, 2025).

[2] C. Singaram, “How do segways self-balance?,” Medium, https://chendurs.medium.com/how-do-segways-self-balance-bbc32ccefdea (accessed Apr. 3, 2025).

[3] T. Harris, “How segways work,” HowStuffWorks Science, https://science.howstuffworks.com/transport/engines-equipment/ginger.htm (accessed Apr. 3, 2025).

[4] “Ninebot,” Segway, https://ap-en.segway.com/mini-pro-specification.html (accessed Apr. 3, 2025).